

Lehigh University Lehigh Preserve

Fritz Laboratory Reports

Civil and Environmental Engineering

1973

Ultimate strength of concrete-filled steel tubular beam-columns, February 1973 (73-53)

Glenn P. Rentschler

Wai-Fah Chen

Follow this and additional works at: <http://preserve.lehigh.edu/engr-civil-environmental-fritz-lab-reports>

Recommended Citation

Rentschler, Glenn P. and Chen, Wai-Fah, "Ultimate strength of concrete-filled steel tubular beam-columns, February 1973 (73-53)" (1973). *Fritz Laboratory Reports*. Paper 2080.
<http://preserve.lehigh.edu/engr-civil-environmental-fritz-lab-reports/2080>

This Technical Report is brought to you for free and open access by the Civil and Environmental Engineering at Lehigh Preserve. It has been accepted for inclusion in Fritz Laboratory Reports by an authorized administrator of Lehigh Preserve. For more information, please contact preserve@lehigh.edu.

ULTIMATE STRENGTH OF CONCRETE-FILLED
STEEL TUBULAR BEAM-COLUMNS

by

Glenn P. Rentschler¹ and Wai F. Chen²

1. INTRODUCTION

In analysis of concrete-filled steel tubular beam-columns, several procedures have been introduced. Knowles and Park (7) presented a method for determining the buckling load of axially loaded columns by adding the tangent modulus loads of the concrete core and steel tube directly by assuming each to act as independent columns. However, no real column is perfectly straight, without material imperfection or concentrically loaded. Hence, all column problems must be treated as beam-columns (deflection problems), not as straight columns (eigenvalue problems, tangent modulus method). The 1971 ACI Building Code (1) now requires a minimum eccentricity of thrust for the design of all concrete compression members. All columns, therefore, are really designed as beam-columns.

For beam-columns several deflection approaches have been taken to determine more exact solutions. Neogi, Sen, and Chapman (8) used a Column Deflection Curve method where deflection as a variable to solve the more realistic beam-column problem. This theory was simplified by Chen and Atsuta (2) in the Column Curvature Curve method (with application toward concrete-filled steel tubular beam-columns by Chen and Chen (5)) where curvature is used as a variable. Both these methods, although providing accurate and reliable results, are cumbersome in that extensive computer programs are required.

¹Research Assistant of Fritz Laboratory, Lehigh University, Bethlehem, Pa.

²Associate Professor of Civil Engineering, Fritz Laboratory, Lehigh University, Bethlehem, Pa.

For actual design of concrete-filled steel tubular beam-columns, a simple method of computing the relationship of maximum bending moment to maximum axial load for a given cross-section, length, loading, and end conditions is very important. Several researchers (6,7) have proposed over simplified bending moment-axial load interaction formulas. These interaction formulas, although most are on the conservative side, lean too far in that direction to be used as a basis of economical design.

The work presented in this paper is an effort to present a simplified, yet sufficiently accurate, procedure, which may be used in design offices without extensive computer facilities, for determining the ultimate strength of concrete-filled steel tubular beam-columns. This procedure is based on several assumptions related to concrete strength, steel strength, and moment-curvature-thrust relationship.

The method presented here is related to work done by Chen and Atsuta (4) on simple interaction equations for steel beam-columns. The results computed using this procedure will be compared with the more exact computer based solution of Chen and Chen (5).

2. BASIC CONCEPTS

2.1 Concrete and Steel Property Idealizations

In a report by Chen and Chen (5) concerning the analysis of concrete-filled steel tubular beam-columns by a computerized column curvature curve method, the effect of three different concrete

stress-strain relationships on the strength of these sections was investigated. These concrete relationships are shown in Fig. 1.

In this figure, Curve 1 assumes the uniaxial state of stress; Curve 2 represents the triaxial state of stress, the effect being assumed to increase only the ductility and not the strength; Curve 3 depicts also the triaxial state of stress, the effect being assumed to increase both the strength and ductility of the concrete.

Based on the results of this previous research, it was concluded that there is no significant difference among the three assumed concrete curves on the ultimate strength of concrete-filled steel tubular beam-columns. On this basis, the concrete stress-strain relationship will be assumed to be the bilinear form shown in Figure 2(a). This curve corresponds to a simplified triaxial state of stress where the effect is only to increase the ductility. The modulus of elasticity for concrete (E_c) in the linear elastic range will be based on the American Concrete Institute (1) formula:

$$E_c = 33\omega^{1.5} \sqrt{f'_c} \quad (1)$$

where ω = the density of concrete in pounds per cubic foot and f'_c = the compressive strength of standard concrete cylinders in pounds per square inch. It will be assumed that concrete exhibits no tensile strength.

For steel, the linear elastic-perfectly plastic form shown in Figure 2(b) will be assumed. The modulus of elasticity (E_s) up to the yield stress (f_y) for steel will be taken to be 31,000,000 pounds per square inch.

2.2 Generalized Moment-Curvature-Thrust Relationship

A general moment-curvature-thrust curve of a concrete-filled steel tubular beam-column section has the shape shown diagrammatically in Figure 3. The curve presents the relationship between bending moment and curvature for a constant value of axial force on a column segment. The precise values associated with this curve can be computed exactly by computer and this has been done for several composite sections by Chen and Chen (5).

The curve in Figure 3 has been non-dimensionalized with respect to the quantities M_o , P_o , and ϕ_o . M_o is the ultimate bending moment when no axial thrust is present; P_o is the ultimate axial force when there is no bending moment present; ϕ_o is the maximum curvature present when M_o is achieved in a section.

Thus, the following identities are defined:

$$m = \frac{M}{M_o}, \quad p = \frac{P}{P_o}, \quad \varphi = \frac{\phi}{\phi_o} \quad (2)$$

where M , P , and ϕ are respectively the bending moment, axial thrust and curvature present in a section at any given time.

The m - p - φ curve of Figure 3 can be divided into two different regions. They are an elastic region and a plastic or work hardening region. The two regions are separated by the point (m_1, φ_1) . The ultimate bending moment and ultimate curvature are called m_{pc} and φ_{pc} respectively. The value of m_{pc} is theoretically only attained at infinite curvature. However, due to strain hardening of steel tube and confinement of concrete, m_{pc} will be attained at a finite curvature φ_{pc} .

The elastic portion of the m - p - ϕ curve varies linearly from zero to (m_1, ϕ_1) , which is the point of initial yield in the cross-section. Initial yield is defined as the value of moment and curvature for a given axial thrust at which the stress in either the steel or concrete fiber farthest from the neutral axis first reaches its yield value, considering only the compressive fiber for concrete. The slope of this linear elastic portion is called the stiffness of the composite section and is defined as

$$EI = \frac{M_1}{\phi_1} \quad (3)$$

or in nondimensionalized form as

$$EI = \frac{M_o m_1}{\phi_o \phi_1} \quad (4)$$

From this point, the rate of change of curvature with respect to bending moment in the plastic region is increasing due to further yielding of the cross-section, the rate being near infinity when m_{pc} is achieved. The term m_{pc} is defined as the moment when the entire cross-section has fully yielded.

Two different cross sections will be utilized in this paper. They are the square and circular tubular sections shown respectively in Figure 6 and Figure 7. Also shown are properties associated with concrete and steel strength.

By examining the m - p - ϕ curves, it is evident that the points m_1, ϕ_1, m_{pc} , and ϕ_{pc} are strictly a function of p . Noticing this

possible relationship, Chen and Chen (5) have derived equations for each of the above four quantities. For example, the equation for m_1 for the square section of Figure 6 is

$$m_1 = (1.0 - p) (0.84 + 2.086p - 4.857p^2) \text{ for } p \leq 0.3$$

and $m_1 = 1.03 (1.0 - p) \text{ for } p \geq 0.3$ (5)

These equations are based on using the concrete stress-strain diagram of Curve 1 in Figure 1.

Similar relationships to Equation 5 have been derived for the other quantities of both the square and the circular sections and are presented in Table 1. These equations are valid only for the particular square and circular sections shown in Figures 6 and 7. The equations in Table 1 will be used as examples in a later portion of this paper in predicting the ultimate strength of concrete-filled steel tubular beam-columns.

2.3 Idealized Moment-Curvature-Thrust Relationship

For a constant thrust, the moment-curvature relationship is assumed to be linear up to a certain level m_{mc} , called the average flow moment. At this point, the section is assumed to flow plastically at the constant bending moment m_{mc} . The idealized and non-dimensionalized moment-curvature-thrust relationship is shown in Figure 3 superimposed upon the exact m - p - ϕ curve. This assumption was used successfully by Chen and Atsuta (4) in solving interaction equations for steel columns.

By using the assumed bilinear moment-curvature-thrust relationship, the maximum bending moment of the m - p - ϕ curve is now considered

to be equal to m_{mc} . The significance of this is that by equating the maximum moment in the beam-column to the average flow moment m_{mc} , the beam-column is assumed to fail by elastic buckling which greatly simplifies, but does not deter greatly from the accuracy of, the solution for ultimate strength.

2.4 Upper and Lower Bounds on Ultimate Strength

The ultimate strength of the composite beam-column is directly related to the value of m_{mc} which lies somewhere between the lower limit m_1 and the upper limit m_{pc} . The satisfactory selection of the average flow moment will lead to an excellent prediction of the beam-column ultimate strength.

2.5 Estimation of the Average Flow Moment

Since the value of the average flow moment m_{mc} must be between m_1 and m_{pc} for all beam-columns, it may be expressed as

$$m_{mc} = m_{pc} - f (m_{pc} - m_1) \quad (6)$$

where f is a parameter used to account for boundary conditions, slenderness effect ℓ/t , and the thrust ratio p . If $f = 0$, the expression reduces to $m_{mc} = m_{pc}$ which is the upper bound solution. If $f = 1$, the expression is $m_{mc} = m_1$, which corresponds to the lower bound solution.

The parameter f will be considered to be a function of three different variables. They are p , ℓ/t , and boundary conditions. This can be expressed as

$$f = f_1 (p, \ell/t) f_2 (\text{B.C.}) \quad (7)$$

where f_1 combines the effects of p and ℓ/t and f_2 accounts for boundary conditions. The choice of the function f will be described later.

3. EXAMPLES

In order to further explain the concept set forth in the previous section, the beam-column with hinged ends having axial force P and equal and opposite end moments M_e will be described (see Fig. 4).

The general solution of this type of beam-column problem giving the ultimate nondimensionalized moment m_e which may be applied at the ends is given by the following formulas (4)

$$\text{if } \chi \leq \cos kl \quad m_e = m_{mc} \quad (8)$$

$$\text{if } \chi \geq \cos kl$$

$$m_e = m_{mc} \frac{\sin kl}{\sqrt{\sin^2 kl + (\chi - \cos kl)^2}} \quad (9)$$

$$\text{where } k^2 = \frac{P}{EI} = \frac{P_o p \phi_o \phi_1}{M_o m_1} \quad (10)$$

or

$$k\ell = \sqrt{\frac{P_o p \phi_o \phi_1 t^2}{m_1 M_o}} \left(\frac{\ell}{t}\right) \quad (11)$$

χ is the ratio of the smaller to the larger end moment with a positive value indicating single curvature.

The values of P_o , M_o and ϕ_o used in calculations are taken from Reference 5. The values for m_1 , ϕ_1 , and m_{pc} are taken from Table 1.

It will be shown later how these section property dependent values may be derived directly by hand calculation.

The upper bound ($f = 0$) and lower bound ($f = 1$) solutions are obtained by substituting m_{pc} and m_1 , for m_{mc} in turn into Equation 8 or 9. This is done for $\lambda/t = 20$ and the square composite section in Figure 4.

Considering the effect of the axial load ratio $\frac{P}{P_o} = p$, if $p = 0$, the problem reduces to a beam problem and the fully plastic moment $m_{pc} = m_{mc}$ will control the ultimate strength, i.e., $f = 0$. If $p = 1$, the problem is one of an axially loaded short column and the initial yield moment $m_1 = m_{mc}$ will be the controlling value, i.e., $f = 1$. Thus the real solution for m_{mc} should be near m_{pc} for small values of p and approach m_1 for larger values of p . The exact solution plotted in Figure 4 depicts this fact clearly.

Therefore, the solution of f , will be assumed to be of the form

$$f_1 \left(\frac{P}{P_o} \right) = P^N \quad (12)$$

Initially a simple value of $N = 1$ for $\lambda/t = 20$ in Figure 4 was tried. From this plot, it is evident that this curve has the same shape as the exact solution but is slightly in error. After further trials of values of N , it was found that a value of $N = 0.63$ obtained results which are in very close agreement to the exact solution.

This same curve fitting procedure was used for several values of ℓ/t to find which value of N provided the most precise results when compared with the exact solution for that particular ℓ/t . From this procedure, it was found that there existed a relationship between N and ℓ/t . The relationship is

$$N = \frac{460.0}{(\ell/t)^{2.2}} \quad (13)$$

This function is presented graphically in Figure 5. Also shown in Figure 5 are the other two trial functions of N . Although the three functions appear to differ significantly, the functions $N = 1$ and $N = 1.0 - 0.02 \ell/t$ give interaction curves which do not differ appreciably from the true curves. This has been illustrated in Figure 4 and later in Figure 6 (the curves corresponding to $N = 1.0 - 0.02 \ell/t$ are very close to the exact curves. For clarity, the curves are not plotted in the figures). This shows that although Equation 13 provides the most precise solution, the simpler functions of $N = 1$ or $N = 1.0 - 0.02 \ell/t$ may be used if accuracy may be slightly sacrificed.

In applying the same procedure described above for the circular section, it was found that the same function of N as given by Equation 13 also provided very good agreement with the exact solution (see Fig. 7).

Throughout the above analysis, it was assumed that $f_2 = 1.0$. A proof that this assumption was valid for hinge-ended columns will now be demonstrated. This parameter is a function of boundary conditions. Take, for example, the uniformly loaded beam-columns in Figure 8. If a beam-column has fixed ends as shown in Figure 8(b), plastic hinges

will form first at the ends as shown. The third and last plastic hinge will form at C but until this is accomplished, large rotations will be experienced at A and B, the previously formed plastic hinges. At the ultimate state, the moments at the ends A and B will be close to m_{pc} and the moment at the center C will be close to m_1 . Therefore m_{mc} may be taken as the mean value of m_{pc} and m_1 and therefore f_2 (fixed) will be taken to be 0.5. However, if the beam-column is simply supported as in Figure 8(a), the only hinge to form occurs at the center and therefore the initial yield moment m_1 , will be taken as the governing flow moment or f_2 (hinged) = 1.0.

4. THEORETICAL DERIVATIONS

To accurately calculate the ultimate strength of concrete-filled steel tubular beam-columns, several quantities which are dependent on cross-section properties are needed as shown in the previous sections. These quantities are m_1 , m_{pc} , M_o , P_o , and EI . Values of these quantities used in the preceding examples were taken from Reference 5 where they were calculated by computer techniques.

Herein, the calculation of m_1 , m_{pc} , M_o , P_o , and EI by simplified procedures will be explained. Involved in this computation will be the use of the material property assumptions as shown in Figure 2. Both rectangular (square) and circular cases will be discussed as these are the two primary geometric shapes used in concrete-filled steel tubular beam-columns. Two specific sections along with properties of the sections are given in Figures 9 and 10. Hereafter,

the term rectangle will be used for Figure 9(a) as a square is a particular case of a rectangle.

4.1 Calculation of P_o

The quantity P_o is the ultimate axial force on the composite beam-column when there is no bending moment present and instability effects are neglected. This quantity may be expressed as

$$P_o = f_y A_s + 0.85 f'_c A_c \quad (14)$$

where A_s and A_c are the steel and concrete areas respectively and are equal to the following for the particular section involved:

$$\text{Rectangular: } A_s = b_1 d_1 - b_2 d_2 \quad (15a)$$

$$A_c = b_2 d_2 \quad (15b)$$

$$\text{Circular: } A_s = \pi (r_o^2 - r_i^2) \quad (16a)$$

$$A_c = \pi r_i^2 \quad (16b)$$

The quantities b_1 , d_1 , b_2 , d_2 , r_o , and r_i are defined in Figs. 9 and 10.

4.2 Calculation of m_{pc} and M_o

The quantity m_{pc} is the ultimate bending moment on a cross-section with varying amounts of axial force under the condition that all material are fully yielded, whether in tension or compression.

Rectangular Section

The rectangular composite section of Figure 9(a) will be treated to be equivalent to the sum of the section components as shown in Figures 9(b,c, and d). This procedure greatly simplifies computation

as the composite section is now decomposed into simple solid rectangles. Each of these components may be treated as shown in Figure 9(e), depicting the neutral axis and the compressive and tensile areas for each of the three components.

The term A_1 of Figure 9(e) refers to the compressive area of the total steel area shown in Figure 9(a), while A_2 refers to the compressive area of either the steel or concrete areas shown in Figures 9(c and d). The terms e_1 and \bar{e}_1 refer to the location of the neutral axis and the centroid of the compressive area respectively of the total area shown in Figure 9(b), while e_2 and \bar{e}_2 are similarly defined for areas of Figure 9(c and d). All values of e are measured from point o as shown in Figure 9(e) with regard to sign.

The quantities e_1 and e_2 are the same as long as the distance of the neutral axis from o does not exceed $\frac{d_2}{2}$. When e_1 exceeds $\frac{d_2}{2}$, e_2 remains a constant value of $\frac{d_2}{2}$.

The resultant axial force and bending moment on the composite section can now be expressed as

$$P = f_y (A_T - 2 A_1) - f_y (A_c - 2 A_2) - \alpha f'_c A_2 \quad (17)$$

$$M_{pc} = 2 A_1 f_y \bar{e}_1 - 2 A_2 f_y \bar{e}_2 + A_2 \alpha f'_c \bar{e}_2 \quad (18)$$

in which

$$A_T = b_1 d_1, \quad A_1 = \left(\frac{d_1}{2} - e_1\right) b_1, \quad A_2 = \left(\frac{d_2}{2} - e_2\right) b_2 \quad (19)$$

$$\bar{e}_1 = e_1 + \left(\frac{d_1}{4} - \frac{e_1}{2}\right), \quad \bar{e}_2 = e_2 + \left(\frac{d_2}{4} - \frac{e_2}{2}\right) \quad (20)$$

The term α is a factor used to account for the confining effects of the concrete and to approximate the stress distribution for easier computation. This term α is related to the location of the neutral axis as follows

$$\alpha = 0.60 \quad \text{for } |e_1| < \frac{d_2}{2} \quad (19a)$$

$$\alpha = 0.60 + (0.85 - 0.60) \frac{|e_1| - \left(\frac{d_2}{2}\right)}{\left(\frac{d_1}{2}\right) - \left(\frac{d_2}{2}\right)} \quad \text{for } \frac{d_2}{2} \leq |e_1| \leq \frac{d_1}{2} \quad (19b)$$

To find M_o , which is the plastic limit moment when P equals zero, P in Equation 17 is set equal to zero and the location of the neutral axis is found. Once the location is found, these values of e_1 and e_2 are used in Equation 18 to solve for M_o .

Having found M_o and P_o , the quantities M_{pc} and P may be non-dimensionalized by Equation 2 yielding the quantities m_{pc} and p.

Circular Section

The circular composite section will be assumed to be equivalent to the sum of the section components as shown in Figures 10 (b,c and d).

The quantities A_T , A_1 , A_2 , \bar{e}_1 and \bar{e}_2 for the circular section of Figure 10(e) are now equal to

$$A_T = \pi r_o^2 \quad (20a)$$

$$A_1 = r_o^2 \left(\theta_o - \frac{1}{2} \sin 2\theta_o \right) \quad (20b)$$

$$A_2 = r_i^2 \left(\theta_i - \frac{1}{2} \sin 2\theta_i \right) \quad (20c)$$

$$\bar{e}_1 = \frac{1}{2} r_o \frac{\sin \theta_o - \frac{1}{3} \sin 3\theta_o}{\theta_o - \frac{1}{2} \sin 2\theta_o} \quad (20d)$$

$$\bar{e}_2 = \frac{1}{2} r_i \frac{\sin \theta_i - \frac{1}{3} \sin 3\theta_i}{\theta_i - \frac{1}{2} \sin 2\theta_i} \quad (20e)$$

where

$$\theta_o = \cos^{-1} \frac{e_1}{r_o} \quad \text{for } \frac{e_1}{r_o} \leq 1 \quad (21a)$$

$$\theta_i = \cos^{-1} \frac{e_2}{r_i} \quad \text{for } \frac{e_2}{r_i} \leq 1 \quad (21b)$$

Having computed these quantities, they may be substituted into Equations 17 and 18 giving P and M_{pc} as a function of the neutral axis location.

However, for the circular section, α takes the following form

$$\alpha = 0.45 \quad \text{for } |e_1| < 0.9 r_i \quad (22a)$$

$$\alpha = 0.45 + (0.85 - 0.45) \frac{|e_1| - 0.9 r_i}{r_o - 0.9 r_i} \quad \text{for } 0.9 r_i \leq |e_1| \leq r_o \quad (22b)$$

Figures 11 and 12 show the relationship of p to m_{pc} calculated from equations 17 and 18 and from Equations in Table 1. Good agreement is observed.

Calculation of m_1

The quantity m_1 , called the initial yield moment, is defined as the value of moment for a given axial thrust at which the stress

in either the steel or concrete fiber farthest from the neutral axis first reaches its yield value, considering only the compressive fiber for concrete.

The method of computing m_1 as a function of p is straightforward but the procedure may become quite tedious. To simplify the procedure, a factor β , defined as a modified shape factor, will be introduced as

$$\beta = \frac{m_{pc}}{m_1} \quad (23)$$

This term β is analogous to the shape factor in plastic design of steel. However, here β is not constant for a section but is a function of p . The values of β vs. p for both the rectangular and circular concrete-filled steel tubular beam-column are shown in Figure 13. These values are obtained by using the values of m_{pc} and m_1 from Table 1. It can be seen that the value of β may be approximated by the following straight line equation for both rectangular and circular sections:

$$\beta = 1.20 + 0.40p \quad (24)$$

Calculation of EI

The quantity EI may be based on the ACI Formula (1):

$$EI = \left(\frac{E_c I_g}{5} + E_s I_s \right) \quad (25)$$

where I_g = moment of inertia of concrete in a cross section

I_s = moment of inertia of steel in a cross section

5. ACCURACY OF THEORETICAL METHOD

5.1 Comparison with Experimental Results

As a basis for establishing confidence, existing experimental data on ultimate strength of concrete-filled steel tubular beam-columns will be compared with calculations using the procedure described in this paper. The experimental data used for comparison is from tests conducted by Neogi, Sen, and Chapman which are reported in Ref. 8.

The properties of the tested composite columns are given in Table 2. All beam-columns are hinged ended and eccentrically loaded at the ends, with both ends having equal eccentricity bending the beam-column in single curvature.

The tested and computed beam-column strengths are based on both beam-columns having the same bending moment at the hinged ends at failure. The tested ultimate axial load is then compared with the computed axial load. This comparison is shown in Table 2. The computed values are in fairly good agreement with test values and in most cases, the experimental values are on the safe side by achieving value greater than computed.

5.2 Comparison with ACI Moment Amplification Formula

From the ACI Building Code, compression members shall be designed for a computed axial load and for a maximum moment equal to a magnification factor multiplied by the maximum end moment. The magnification factor δ_{aci} is of the form (Ref. 1)

$$\delta_{aci} = \frac{C_m}{1 - \frac{P}{\psi P_c}} \geq 1.0 \quad (26)$$

where $C_m = 0.6 + 0.4 \frac{M_a}{M_b}$

M_a = value of smaller end moment

M_b = value of larger end moment (M_a and M_b are positive if bent in single curvature)

$$P_c = \frac{\pi^2 EI}{(k_1 \ell)^2}$$

P = design axial load

ψ = reduction factor equal to .75 for concrete-filled tubular beam-columns

$k_1 \ell$ = effective length of member between hinges

A similar factor, called δ , may be calculated using the principals described in this paper. The dimensionalized average flow moment, M_{mc} is the maximum moment anywhere along the beam-column length. The term δ may be expressed as

$$\delta = \frac{M_{mc}}{M_e} \quad (27)$$

In Table 3 a comparison is given of δ with δ_{aci} for the beam-columns described in Table 2. For both computations, the same axial load was used, with δ computed on the resulting theoretical end moment, M_e , and average flow moment M_{mc} . It is evident that both values are in good agreement, with the δ_{aci} being on the safe side.

6. SUMMARY AND CONCLUSIONS

A simplified method for calculating the ultimate strength of concrete-filled steel tubular beam-columns has been developed.

This method lends itself to usage without computer facilities and can be subdivided into two distinct computations. The first computation deals strictly with cross-section properties (m_{pc} , m_1 , M_o , P_o and EI) and is not concerned with loading conditions, end conditions, or length. The second computation is concerned with the particular beam-column loading condition, end conditions, and length. To account for these effects, the average flow moment m_{mc} is computed for symmetrical or near symmetrical loading. For significantly unsymmetrical loading cases, m_{mc} is calculated according to Appendix I. The results obtained by the approximate approach are found to be very similar to the computer solution in all cases.

From the comparisons given in Table 2 with experimental results, the procedure for calculating the ultimate strength of concrete-filled steel tubular beam-columns described in this paper besides being simple, is both accurate and safe.

Also, it has been shown that the moment magnification factor given by ACI is a very acceptable and safe method of obtaining the maximum beam-column bending moment given the end moment. Thus, once the maximum end moment is computed by the method discussed in this paper, the maximum moment anywhere in the beam-column may be obtained by using M_{mc} , or conservatively, by using the ACI magnification factor.

7. APPENDICESAppendix I COLUMNS WITH ONLY ONE END MOMENT--LACK OF SYMMETRY

For the unsymmetrically loaded column shown in Figs. 14 or 15, the values of f_1 are found to be

$$f_1 = \begin{cases} 0 & 0 \leq p \leq p_a \\ \frac{p - p_a}{p_b - p_a} & p_a \leq p \leq p_b \\ 1 & p_b \leq p \leq 1 \end{cases} \quad (28)$$

where

$$p_a = \begin{cases} 1 & l/t < 15 \\ \frac{51000}{(l/t)^4} & l/t \geq 15 \end{cases}$$

$$p_b = \begin{cases} 1 & l/t < 18 \\ \frac{1}{0.005 \left(\frac{l}{t}\right)^2 - 0.17 \left(\frac{l}{t}\right) + 2.45} & \frac{l}{t} \geq 18 \end{cases}$$

for square cross sections

and

$$p_a = \begin{cases} 1 & \frac{l}{t} < 12 \\ \frac{1900}{(l/t)^3} & \frac{l}{t} \geq 12 \end{cases} \quad (30)$$

$$p_b = \begin{cases} 1 & \frac{l}{t} < 16 \\ \frac{595}{(l/t)^{2.2}} & \frac{l}{t} \geq 16 \end{cases} \quad (31)$$

for circular cross sections

Using the values of f_1 in Eq. 28 and $f_2 = 1$ for hinged-ended columns, the interaction diagrams for ultimate strength of the square and circular sections are shown in Figs. 14 and 15, respectively. They are seen to be compared favorably with the exact solutions.

Appendix II APPLICATIONS TO VARIOUS BEAM-COLUMN PROBLEMS

Although the discussion presented dealt only with two different beam-columns, application of the concept presented to laterally loaded beam-columns is possible (4).

As was found previously for the symmetric case, the value of m_{mc} for both hinged and fixed ends is

$$m_{mc} = m_{pc} - p^N (m_{pc} - m_1) \quad \text{hinged} \quad (32a)$$

$$m_{mc} = m_{pc} - 0.5 p^N (m_{pc} - m_1) \quad \text{fixed} \quad (32b)$$

where N is given by Equation 13.

Type 1 (Fig. 16a)

The ultimate load w of this beam-column is given by the formula:

$$Q = wL = k M_{mc} kL \frac{\lambda + \cos \frac{kL}{2}}{1 - \cos \frac{kL}{2}} \quad (33)$$

where k^2 is as defined by Equation 10 where

$$\lambda = 0 \text{ for hinged ends}$$

$$\lambda = 1 \text{ for fixed ends}$$

Type 2 (Fig. 16b)

The ultimate load Q is given by:

$$Q = 2k M_{mc} \frac{\lambda + \cos \frac{kL}{2}}{\sin \frac{kL}{2}} \quad (34)$$

Type 3 (Fig. 16c)

The ultimate load for this case of beam-column with partially distributed load is:

$$Q = wC = 2k M_{mc} \frac{\frac{kC}{4}}{\sin \frac{kC}{4}} \frac{\lambda + \cos \frac{kL}{2}}{\sin \left(\frac{kL}{2} - \frac{kC}{4} \right)} \quad (35)$$

As is evident, the previous two types of beam-columns defined by Equations 33 and 34 are particular cases of Equation 35.

In the following two types of beam-columns where there is a lack of symmetry, it is assumed that this unsymmetry is not very large. Thus, M_{mc} defined previously may still be used.

Type 4 (Fig. 16d)

The ultimate concentrated load applied as shown in Figure 16(d) is computed by assuming that the last plastic hinge is formed under the load. It has the form

$$Q = 2k M_{mc} \sin \frac{kL}{2} \frac{\lambda \cos \frac{kL_A - kL_B}{2} + \cos \frac{kL}{2}}{\sin kL_A \sin kL_B} \quad (36)$$

Type 5 (Fig. 16e)

The ultimate load for this beam-column is

$$Q = wC = 2k M_{mc} \frac{\frac{kC}{4}}{\sin \frac{kC}{4}} \sin \left(\frac{kL}{2} - \frac{kC}{4} \right) \frac{\lambda \cos \frac{kL_A - kL_B}{2} + \cos \frac{kL}{2}}{\sin \left(kL_A - \frac{kC}{4} \right) \sin \left(kL_B - \frac{kC}{4} \right)} \quad (37)$$

8. NOMENCLATURE

$A, A_c, A_s, A_1, A_2, A_T$	= area
b_1, b_2, d_1, d_2	= dimensions of rectangular composite section (Fig. 9)
C, Q, w	= load parameters
E_c, E_s	= modulus of elasticity of concrete and steel respectively
EI	= sectional rigidity (Eq. 25)
$e_1, e_2, \bar{e}_1, \bar{e}_2$	= distance from centroid to neutral axis and compressive area respectively (Figs. 9 and 10)
f, f_1, f_2	= parameters defining relationship of m_{mc} to m_1 and m_{pc}
f'_c, f_y	= concrete compressive strength and steel yield strength
I_g, I_s	= moment of inertia of concrete and steel
k	$= \sqrt{\frac{P}{EI}}$
$k_1 \ell$	= effective length
ℓ, L	= beam-column length
M, m	= moment ($m = M/M_o$)
M_o	= ultimate moment when no axial thrust is present
M_A, M_B	= beam-column end moments
N	= parameter relating beam-column length to f_1 (Eqs. 12 and 13)
P, p	= axial force ($p = P/P_o$)
P_a, P_b	= axial force (Appendix I)
P_c	= critical axial load
P_o	= ultimate axial force when no moment is present
r_i, r_o	= dimensions of circular composite section (Fig. 10)

t	= outside diameter of circular composite sections and outside length of side perpendicular to axis of bending for rectangular sections
α	= factor accounting for confining effect of concrete
β	= shape factor (Eqs. 23 and 24)
ϵ_c, ϵ_s	= concrete and steel strain
δ, δ_{aci}	= magnification factor
χ	= percentage of end moment
λ	= factor specifying beam-column end conditions
θ_i, θ_o	= angle between y axis and r_i or r_o (Fig. 10)
Φ, φ	= curvature ($\varphi = \Phi/\Phi_o$)
φ_1, φ_{pc}	= nondimensionalized curvature at initial yield and ultimate
Φ_o	= ultimate curvature when no axial thrust is present
ψ	= reduction factor
ω	= concrete density

9. REFERENCES

1. American Concrete Institute
"Building Code Requirements for Reinforced Concrete", ACI 318-71, ACI Committee 318.
2. Chen, W. F. and Atsuta, T.
"Column Curvature Curve Method for Analysis of Beam-Columns", The Structural Engineer, The Journal of the Institution of Structural Engineers, London, England, Vol. 50, No. 6, June 1972, pp. 233-240.
3. Chen, W. F.
"General Solution of Inelastic Beam-Column Problems", Journal of the Engineering Mechanics Division, ASCE, Vol. 96, EM4, August 1970, pp. 421-441.
4. Chen, W. F. and Atsuta, T.
"Simple Interaction Equations for Beam-Columns", Journal of the Structural Division, ASCE, Vol. 98, No. ST7, July 1972, pp. 1413-1426.
5. Chen, W. F. and Chen, C. H.
"Analysis of Concrete-Filled Tubular Beam-Columns", International Association for Bridge and Structural Engineering, September 1973. To appear.
6. Furlong, R. W.
"Strength of Steel-Encased-Concrete Beam Columns", Journal of the Structural Division, ASCE, Vol. 93, No. ST5, October 1967.
7. Knowles, R. B. and Park, R.
"Strength of Concrete-Filled Steel Tubular Columns", Journal of the Structural Division, ASCE, Vol. 95, No. ST12, December 1969, pp. 2526-2587.
8. Neogi, P. K., Sen, H. K. and Chapman, J. C.
"Concrete-Filled Tubular Steel Columns Under Eccentric Loading", The Structural Engineer, The Journal of the Institution of Structural Engineers, London, England, Vol. 47, No. 5, May 1969.

Table 1

PARAMETER FUNCTIONS FOR CONCRETE-FILLED SECTIONS

(a) Square Section ($M_o = 81.5$ in-K, $P_o = 107$ K)

$$p \leq 0.3$$

$$m_1 = (1.0 - p) (0.84 + 2.086 p - 4.857 p^2)$$

$$\varphi_1 = (1.0 - p) (0.27 + 0.676 p - 1.762 p^2)$$

$$m_{pc} = (1.0 - p) (1.00 + 1.553 p - 0.732 p^2)$$

$$\varphi_{pc} = 1.0 / (1.0 + 3.217 p - 0.048 p^2)$$

$$p \geq 0.3$$

$$m_1 = 1.03 (1.0 - p)$$

$$\varphi_1 = 0.31 (1.0 - p)$$

$$m_{pc} = (1.0 - p) (1.195 + 0.883 p - 0.667 p^2)$$

$$\varphi_{pc} = 0.64 - 0.433 p$$

(b) Circular Section ($M_o = 146.1$ in-K, $P_o = 173.4$ K)

$$p \leq 0.1$$

$$m_1 = 0.84 + 0.1 p \quad \varphi_1 = 0.44$$

$$p \geq 0.1$$

$$m_1 = 0.944 (1.0 - p) \quad \varphi_1 = 0.489 (1.0 - p)$$

$$p \leq 0.3$$

$$m_{pc} = (1.0 - p) (1.0 + 1.178 p - 0.829 p^2)$$

$$\varphi_{pc} = 1.0 / (1.0 + 2.058 p - 0.746 p^2)$$

$$p \geq 0.3$$

$$m_{pc} = (1.0 - p) (1.212 + 0.16 p + 0.179 p^2)$$

$$\varphi_{pc} = 1.0 / (1.642 - 1.398 p + 3.641 p^2)$$

TABLE 2

COMPARISON OF EXPERIMENTAL AND COMPUTED STRENGTHS

Speci- men	Length in	Diameter in	Steel Thickness in	End Eccentri- city	f _y ksi	E _s ksi	Concrete Cube Strength psi	P _{test} kips	P _{comp} kips	$\frac{P_{comp}}{P_{test}}$
1	131	6.67	0.201	1.875	44.8	30016	8060	139.8	111.5	.80
2	131	6.66	0.207	1.500	44.8	30016	7840	157.7	120.1	.76
3	131	6.65	0.223	1.875	42.78	30016	6160	134.9	110.2	.82
4	131	6.63	0.258	1.875	43.23	30016	5510	140.5	124.8	.89
5	131	6.66	0.283	1.875	45.25	30016	4640	146.7	141.0	.96
6	131	6.66	0.287	1.500	45.25	30016	4810	166.0	155.0	.93
7	130	6.65	0.347	1.875	46.82	30016	4790	170.2	175.0	1.03
8	131	5.52	0.378	1.250	39.65	30576	6030	123.2	145.6	1.18
9	131	5.52	0.384	1.250	39.65	30576	3920	123.2	136.6	1.11
10	131	5.55	0.197	1.250	42.56	30016	6180	93.6	80.0	.86

TABLE 3COMPARISON OF δ WITH ACI CODE MAGNIFICATION FACTOR

Specimen	δ_{aci}	δ	$\frac{\delta}{\delta_{aci}}$
1	1.812	1.631	.90
2	1.988	1.741	.88
3	1.688	1.548	.92
4	1.624	1.503	.93
5	1.586	1.477	.93
6	1.705	1.560	.92
7	1.566	1.462	.93
8	1.800	1.623	.90
9	1.791	1.617	.90
10	2.266	1.901	.84

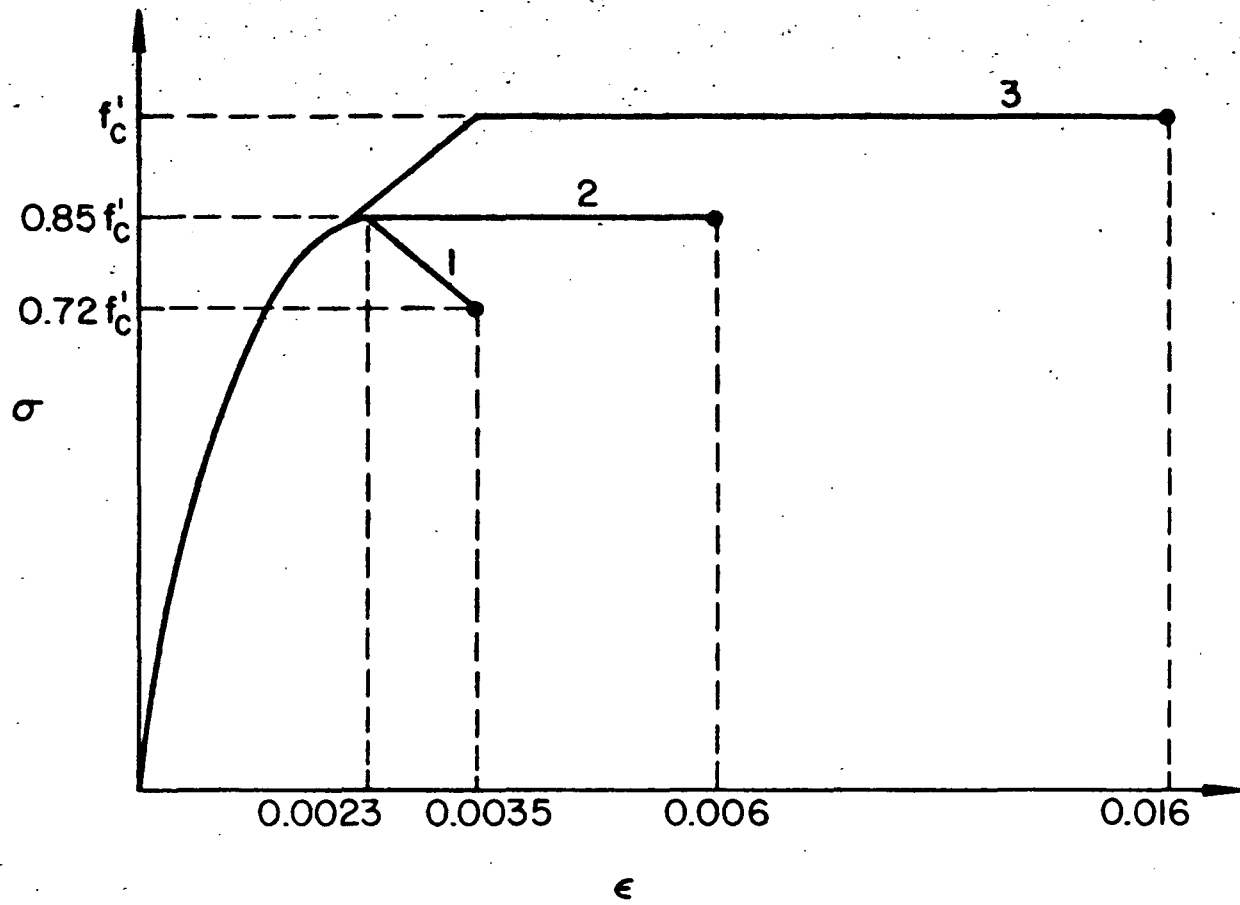
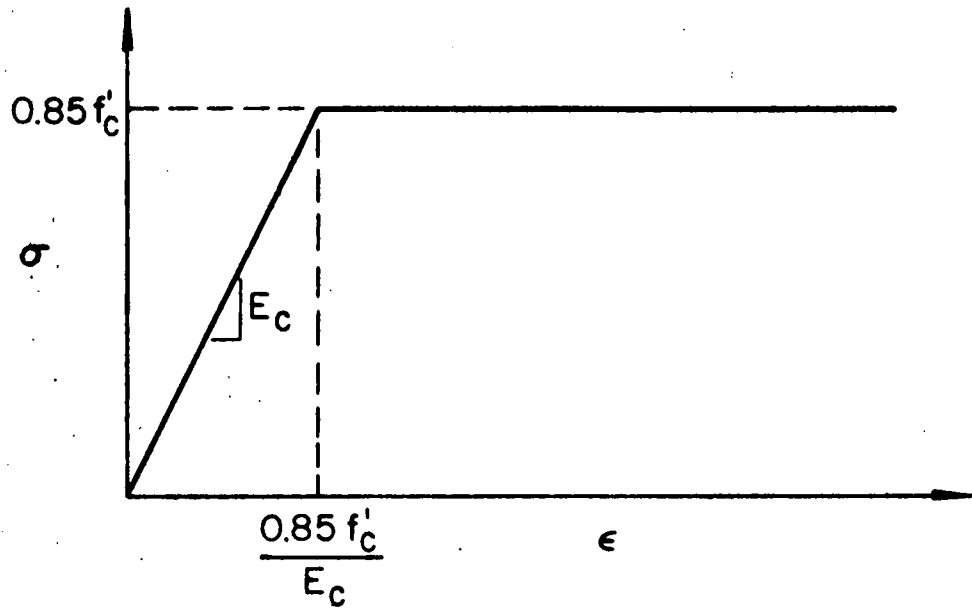
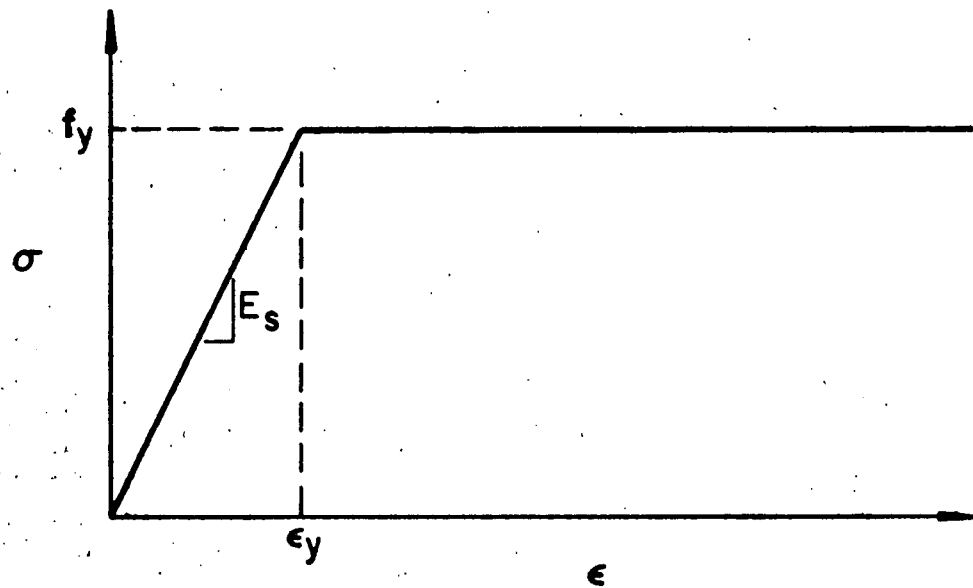


Fig. 1 Three Types of Stress-Strain Relationships of Concrete



a) Idealized Stress - Strain Relation of Concrete



b) Idealized Stress - Strain Relation of Steel

Fig. 2 Idealized Stress-Strain Relationships of Concrete and Steel

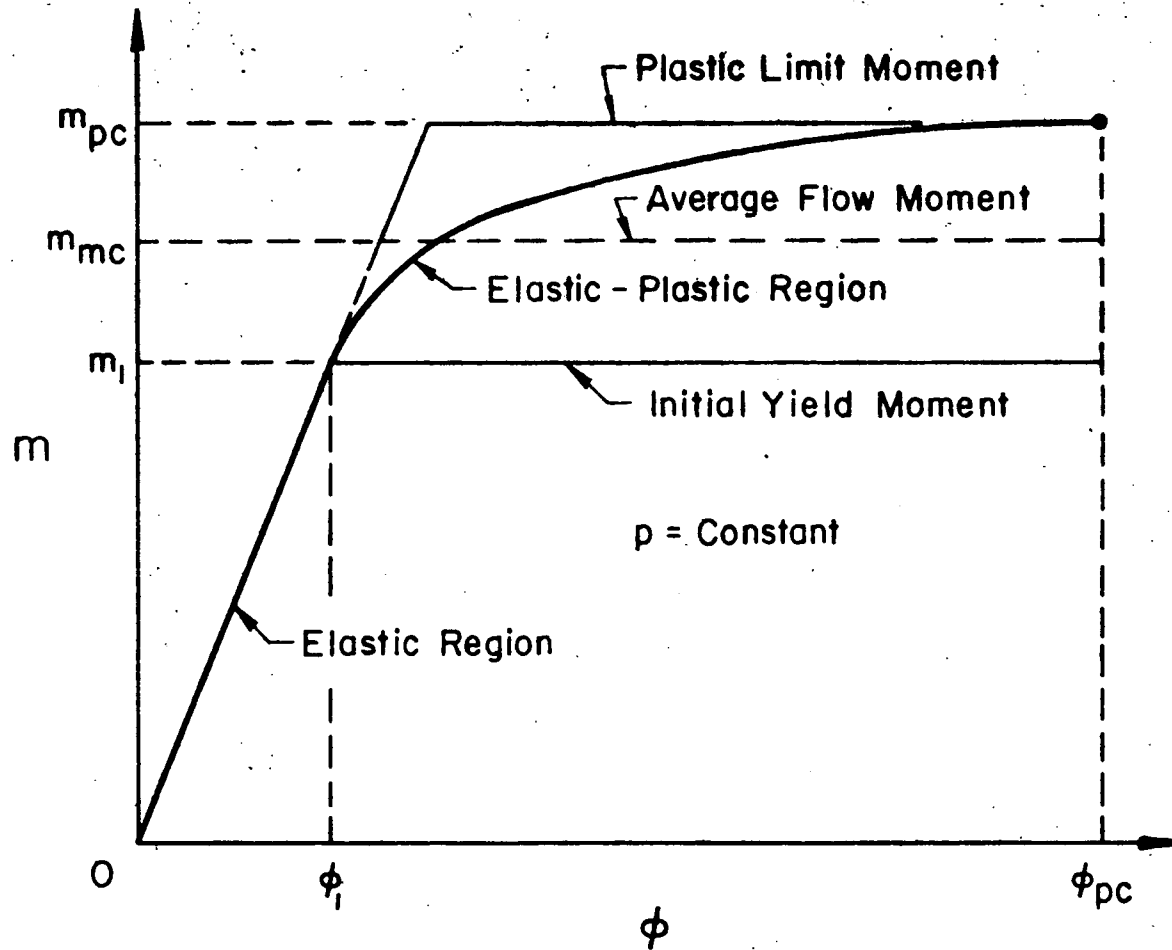


Fig. 3 Idealization of Nondimensionalized Moment-Curvature Relationship

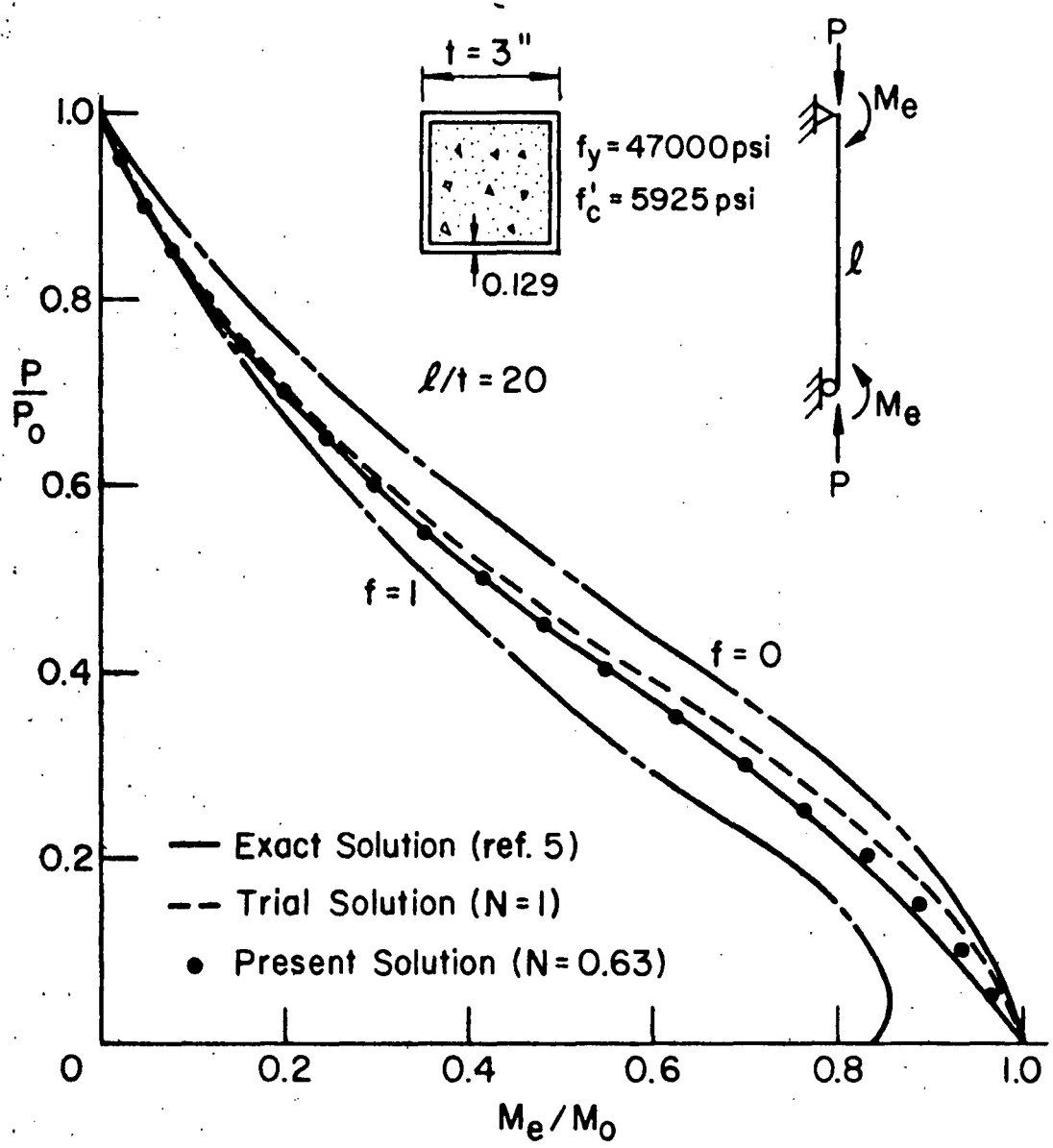


Fig. 4 A Bounded Solution of Beam-Column

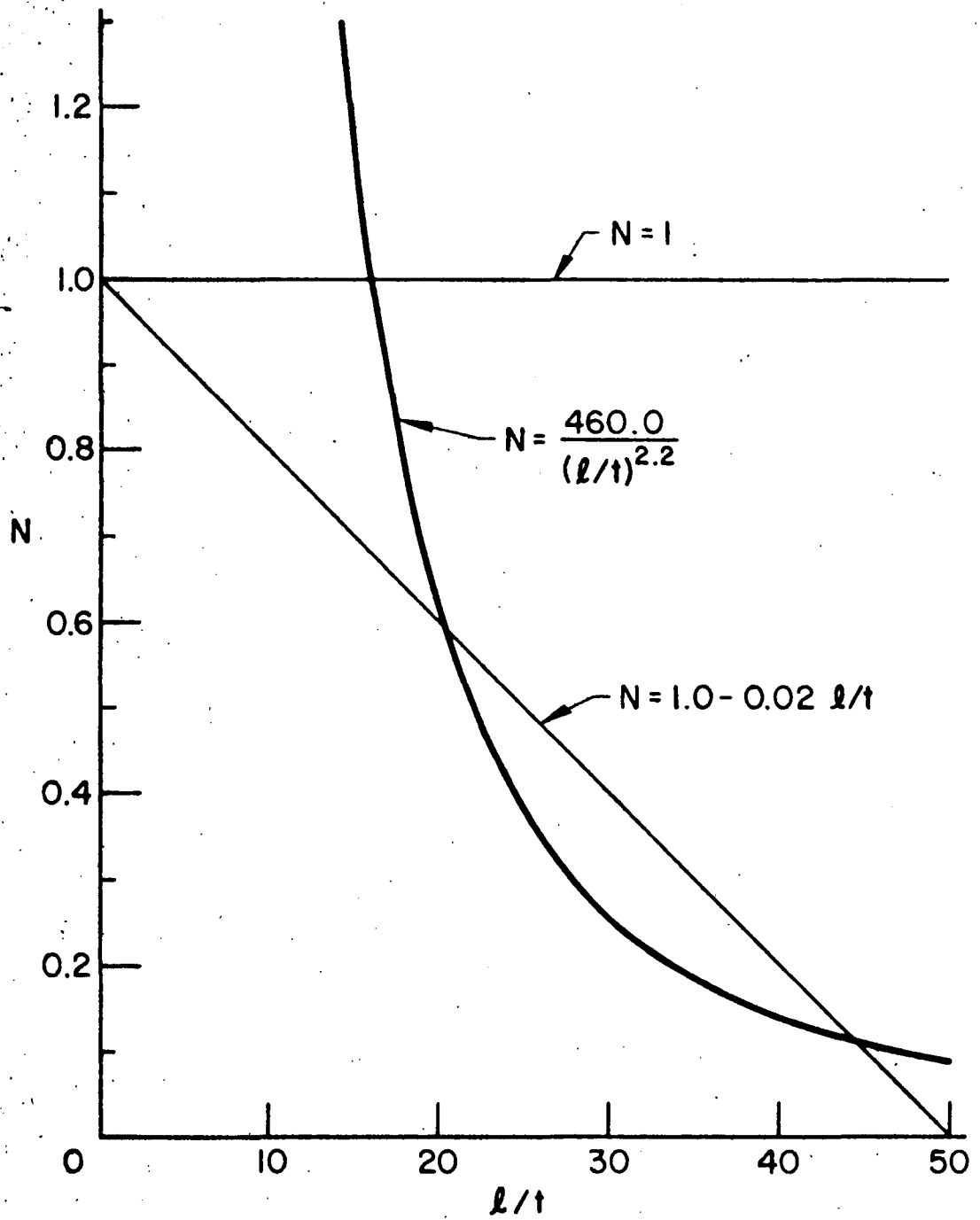


Fig. 5 Three Relationships of N to l/t for $\chi = 1$

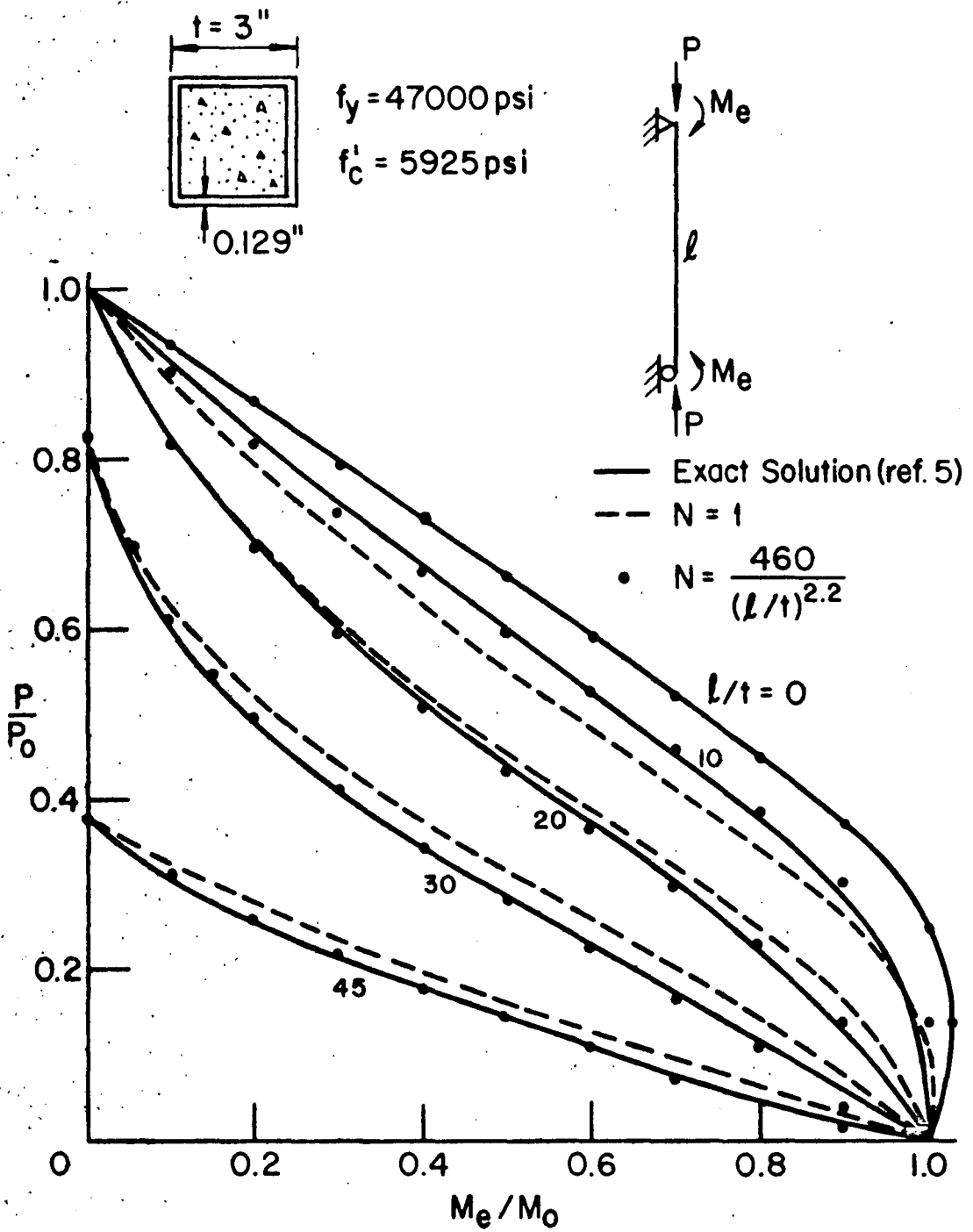


Fig. 6 Interaction Curves with Equal End Moments

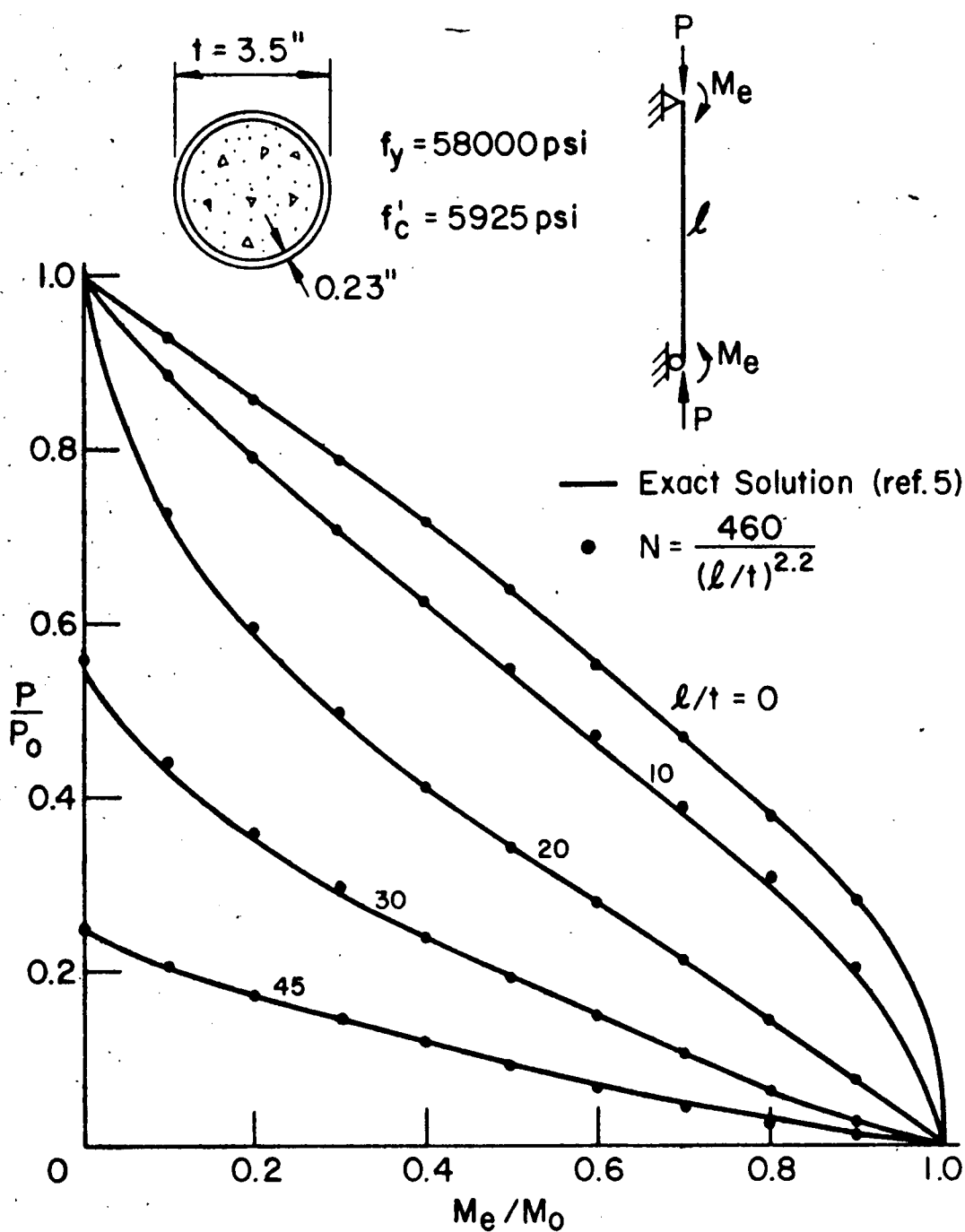
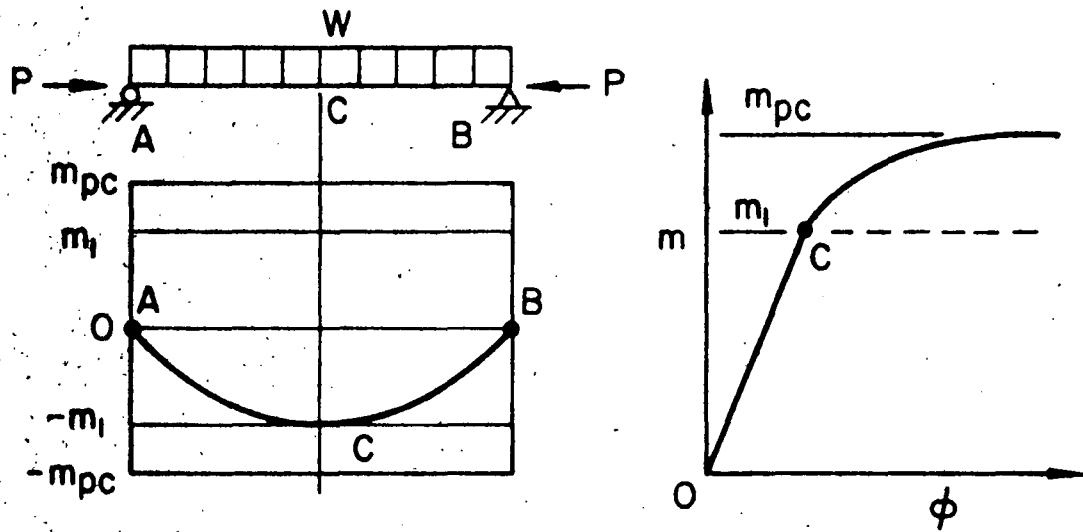
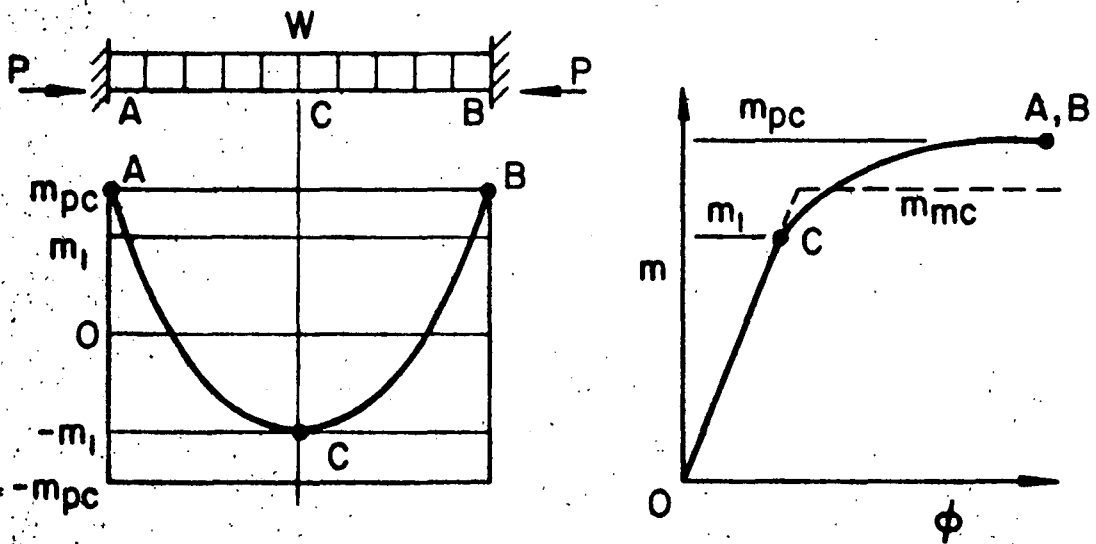


Fig. 7 Interaction Curves with Equal End Moments

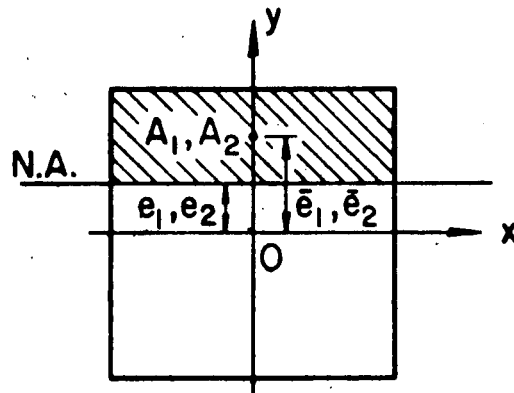
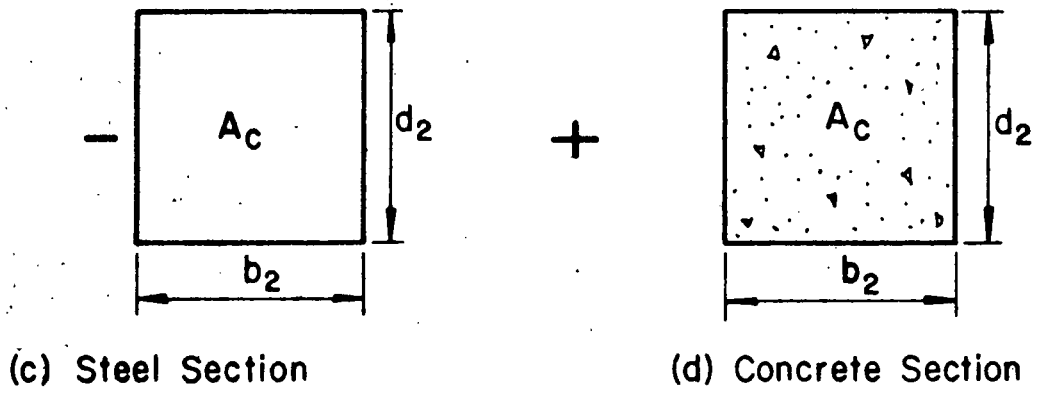
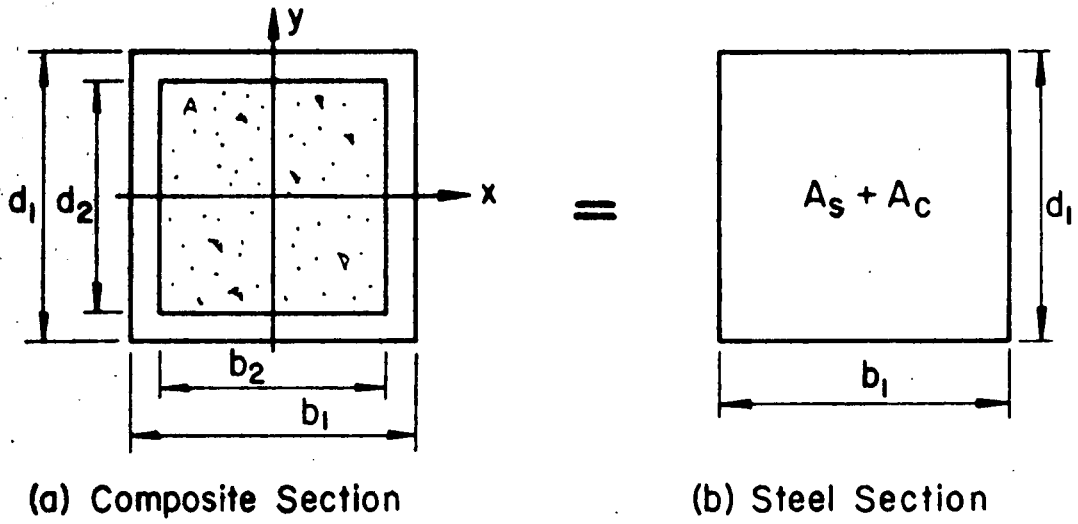


(a) Hinged Ends



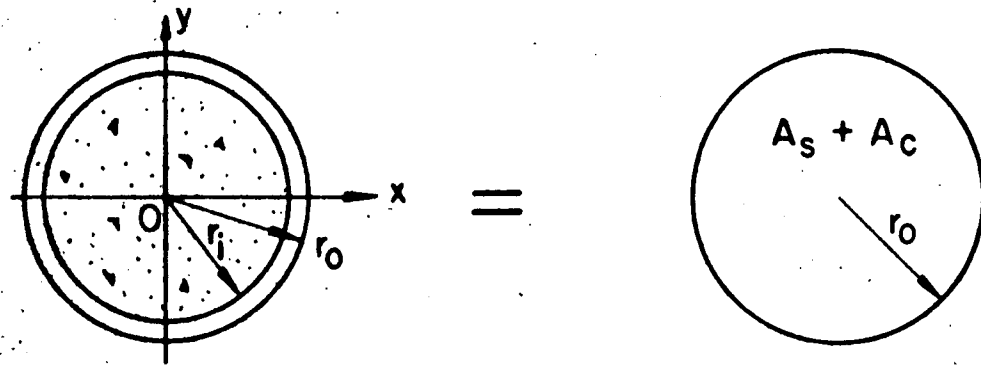
(b) Fixed Ends

Fig. 8 Average Flow Moment of Hinged and Fixed Beam-Columns with Uniform Load



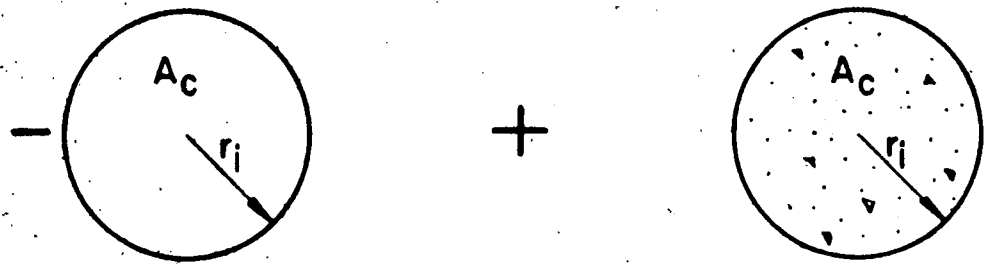
(e) Solid Rectangular Section

Fig. 9 Composite Rectangular Section Characteristics



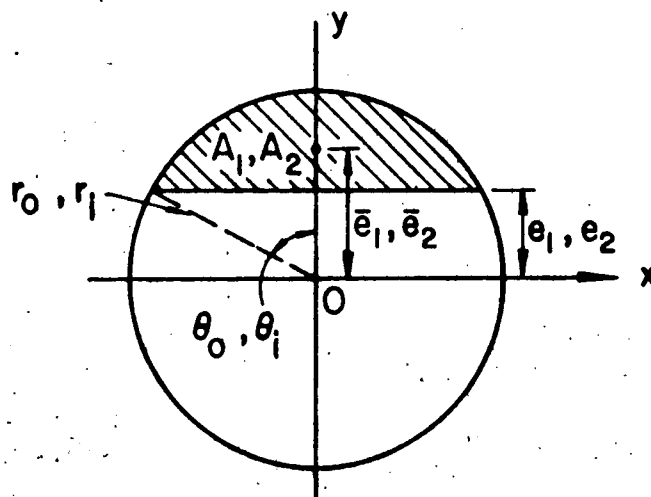
(a) Composite Section

(b) Steel Section



(c) Steel Section

(d) Concrete Section



(e) Solid Circular Section

Fig. 10 Composite Circular Section Characteristics

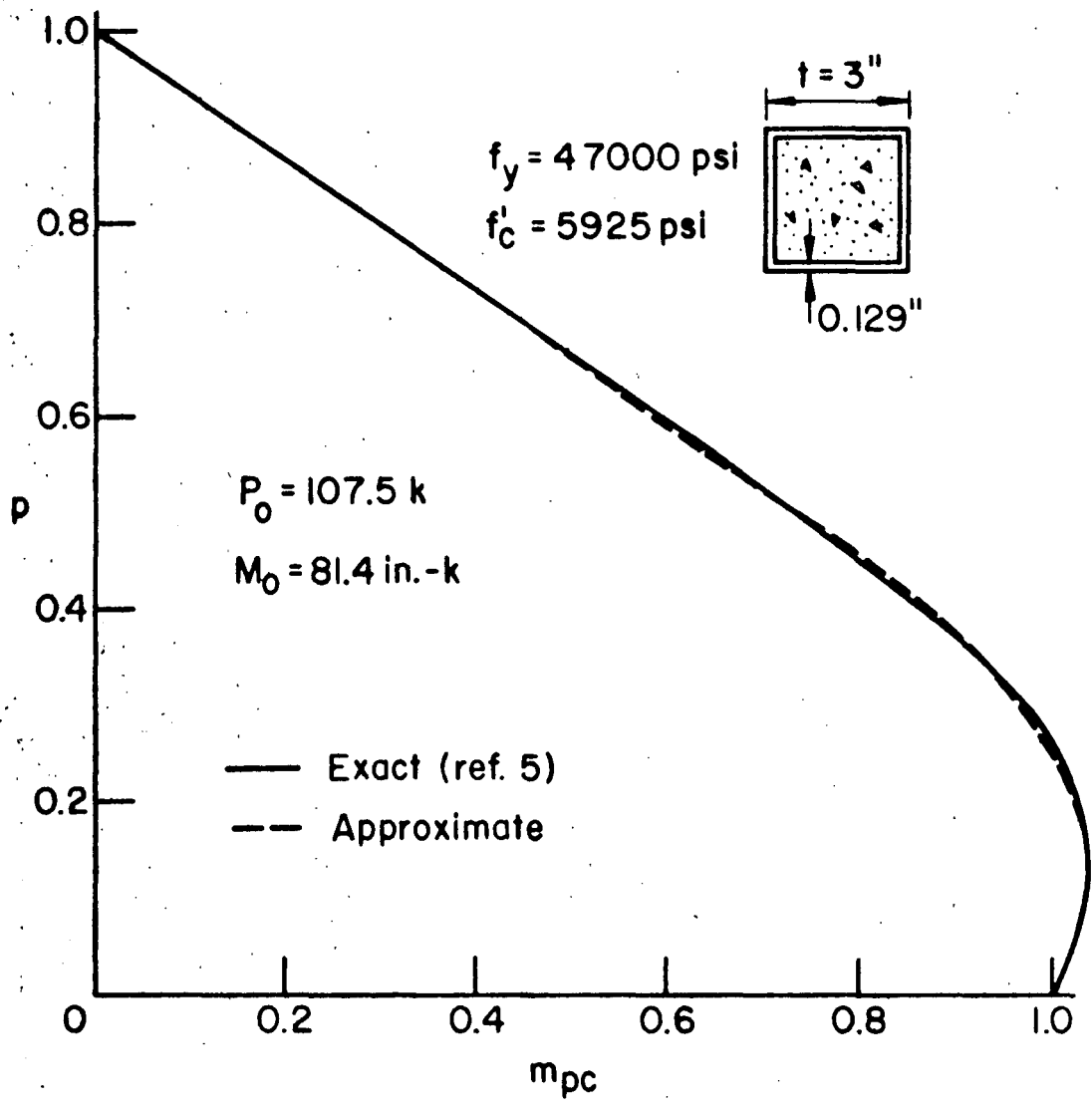


Fig. 11 Relationship of m_{pc} to p for Rectangular Section

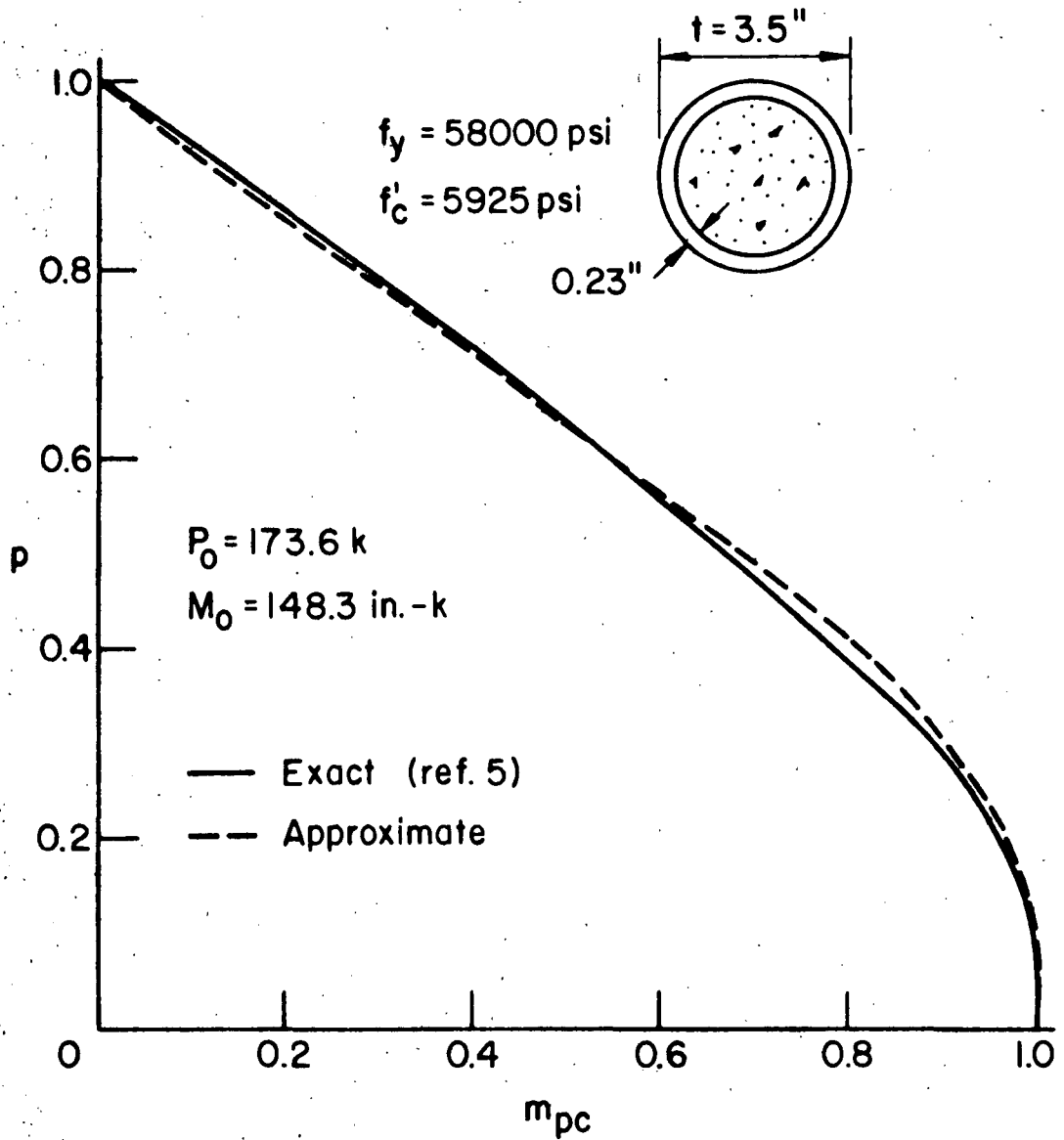


Fig. 12 Relationship of m_{pc} to p for Circular Section

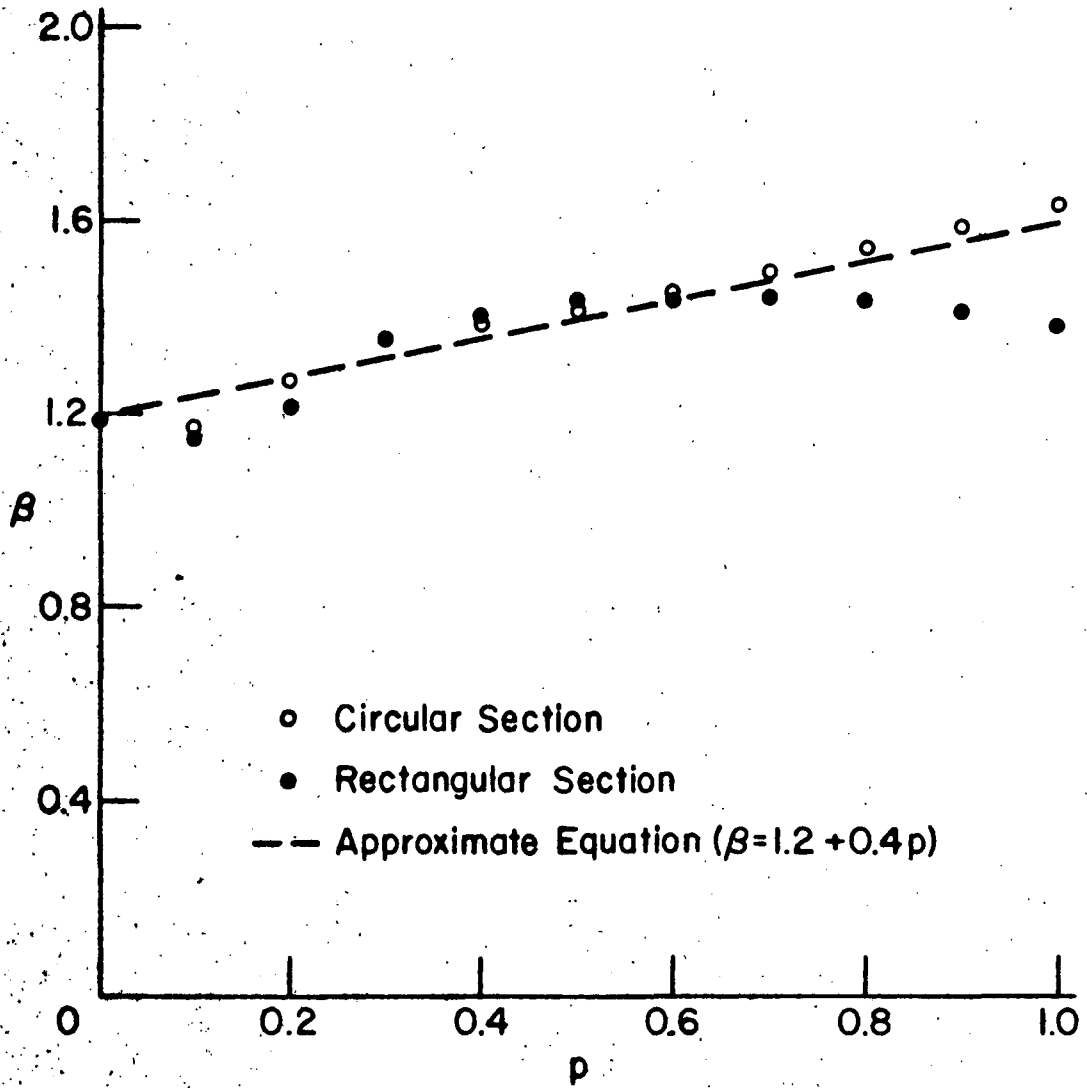


Fig. 13 Relationship of p to β for Rectangular and Circular Sections

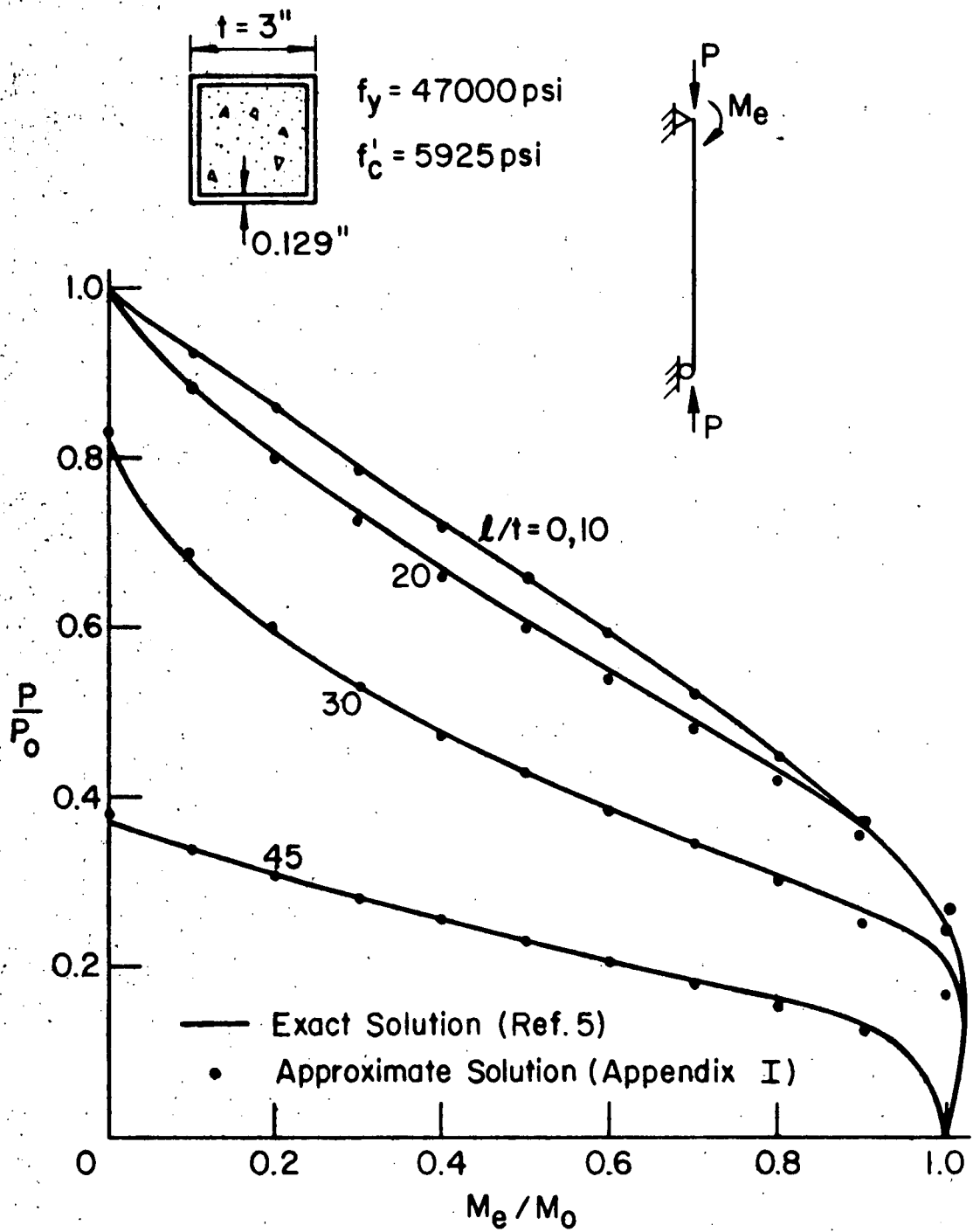


Fig. 14 Interaction Curves with One End Moment

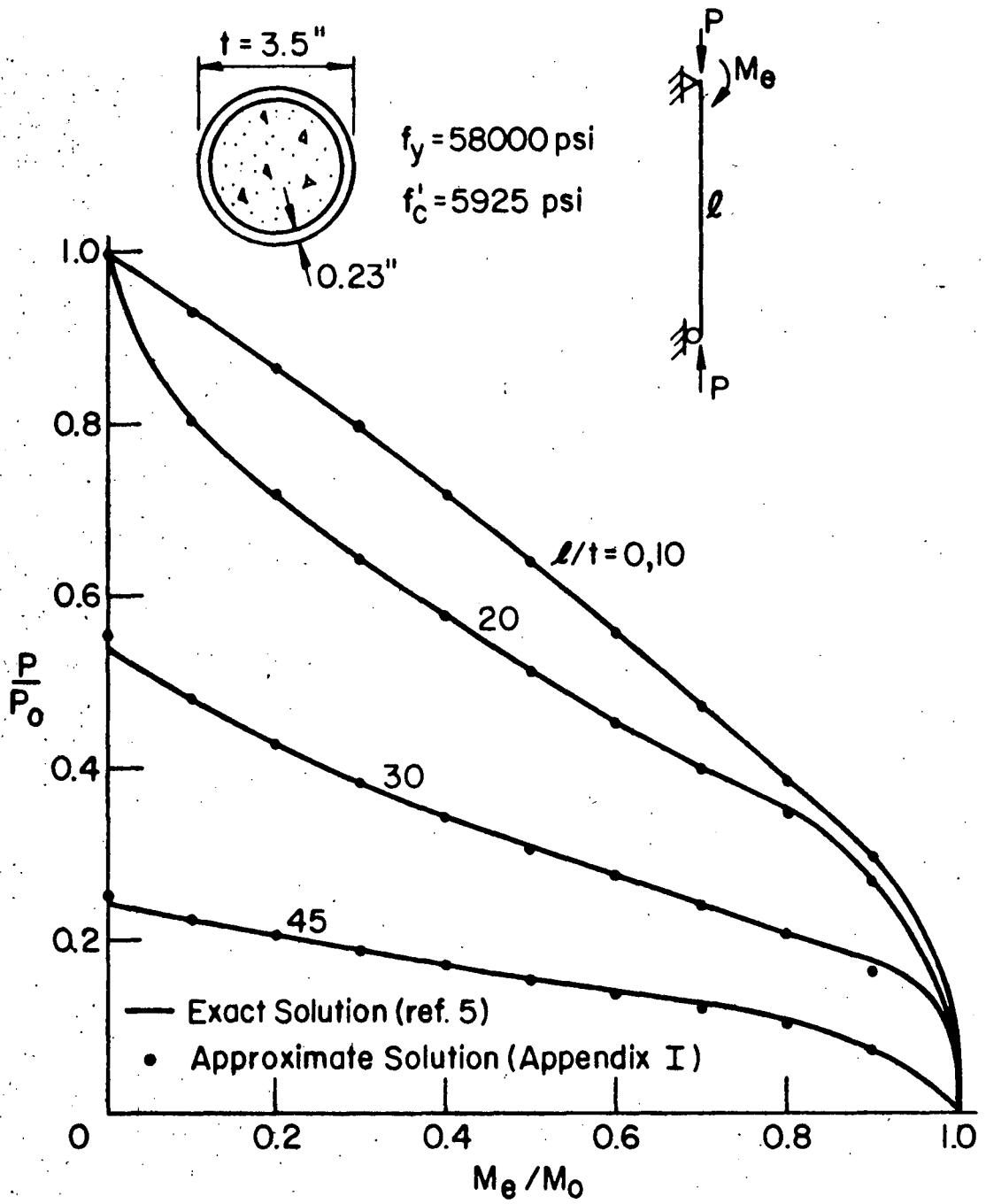


Fig. 15 Interaction Curves with One End Moment

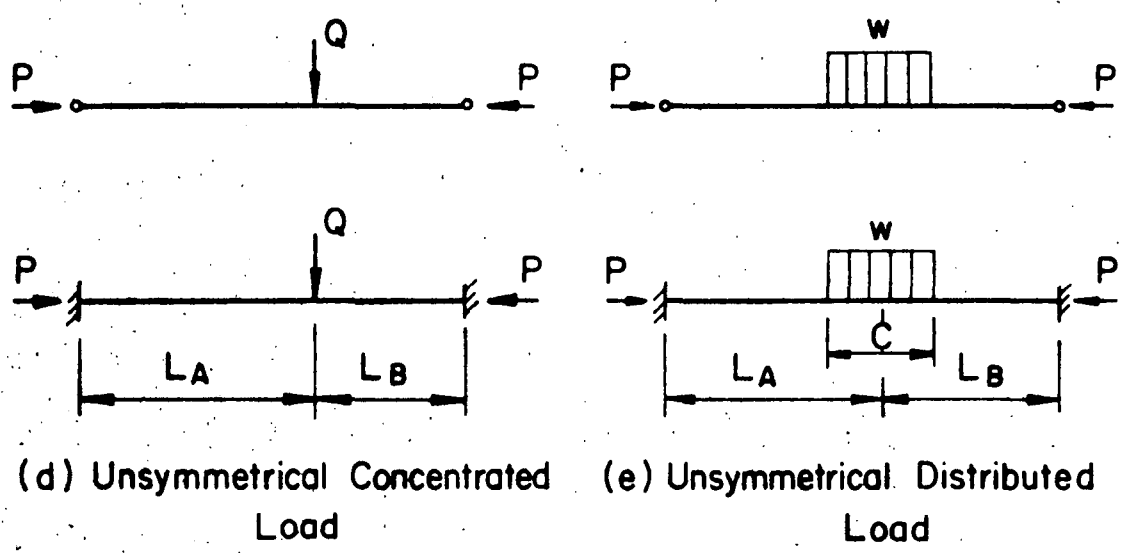
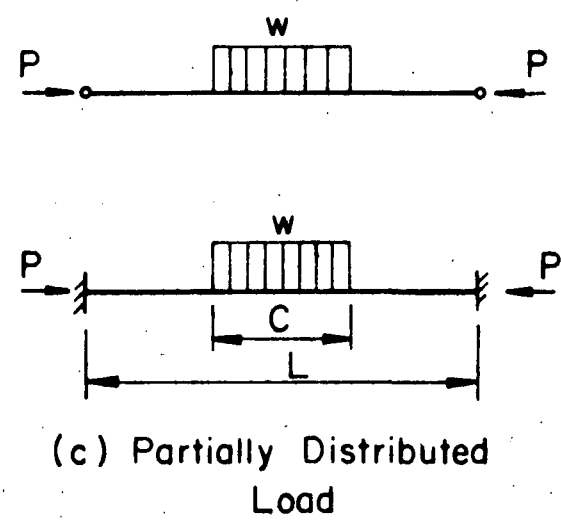
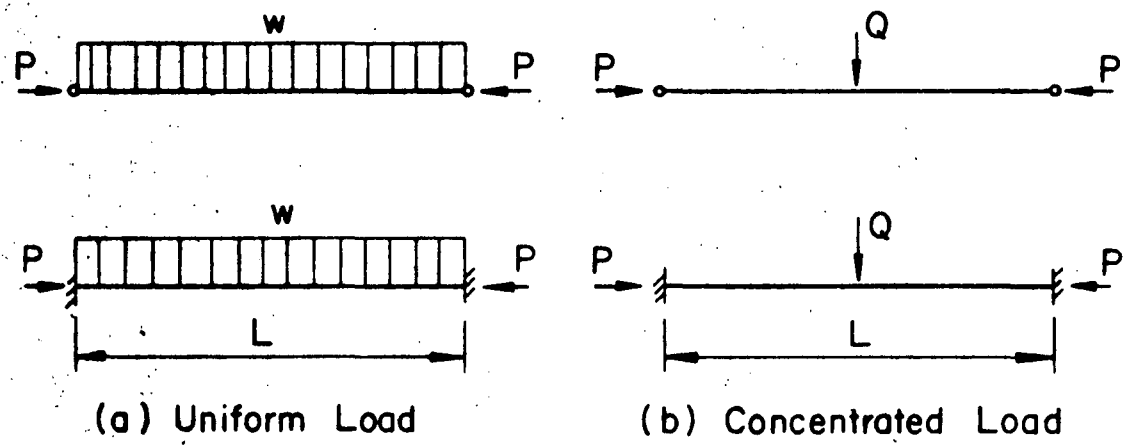


Fig. 16 Laterally Loaded Beam-Columns